2004

NASA FACULTY FELLOWSHIP PROGRAM

MARSHALL SPACE FLIGHT CENTER

THE UNIVERSITY OF ALABAMA
THE UNIVERSITY OF ALABAMA IN HUNTSVILLE
ALABAMA A&M UNIVERSITY

COUPLED ELECTROMAGNETIC RESONATORS FOR ENHANCED COMMUNICATIONS AND TELEMETRY

Prepared By:	Dr. John O. Dimmock
Academic Rank:	Professor
Institution and Department:	The University of Alabama in Huntsville Department of Physics
NASA/MSFC Directorate:	Science
MSFC Colleague:	Dr. David D. Smith

1. Introduction

Future NASA missions will require the collection of an increasing quantity and quality of data which, in turn, will place increasing demands on advanced sensors and advanced high bandwidth telemetry and communications systems. The capabilities of communication and telemetry systems depend, among other factors, on the stability, controllability and spectral purity of the carrier wave. These, in turn, depend on the quality of the oscillator, or resonator, or the Q of the system. Recent work on high Q optical resonators has indicated that the Q, or quality factor, of optical microsphere resonators can be substantially enhanced by coupling several such resonators together.[1-3] In addition to the possibility of enhanced Q and increased energy storage capacity, the coupled optical resonators indicate that a wide variety of interesting and potentially useful phenomena such as induced transparency and interactive mode splitting can be observed depending critically on the morphology and configuration of the microresonators. The purpose of this SFFP has been to examine several different coupled electromagnetic oscillator configurations in order to evaluate their potential for enhanced electromagnetic communications.

2. Coupled LRC circuits

The first such configuration examined was that of three capacitively coupled LRC circuits as shown in Figure 1.

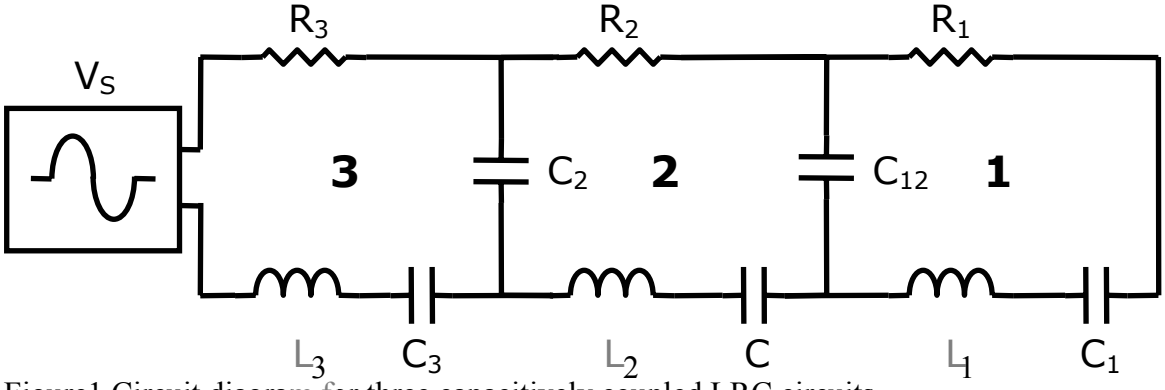

Figure1 Circuit diagram for three capacitively coupled LRC circuits

In this configuration a driving oscillator, connected to circuit 3, produces a voltage input designated as V_S. A general analysis of the voltages and currents in the three circuits was derived for arbitrary values of the inductances L_1, L_2, and L_3, resistances, R_1, R_2, and R_3, circuit capacitances, C_1, C_2, and C_3, and circuit-to-circuit coupling capacitances C_{12}, and C_{23}. It was determined that when the inductances and capacitances are adjusted so that the resonant frequencies of the three individual circuits are the same the coupled circuit displays three separate resonances, one at the common resonant frequency and one higher and one lower frequency split-off resonance. Figure 2 shows the stored energy in each of the three circuits as a function of oscillator frequency for a given selection of circuit parameter values.

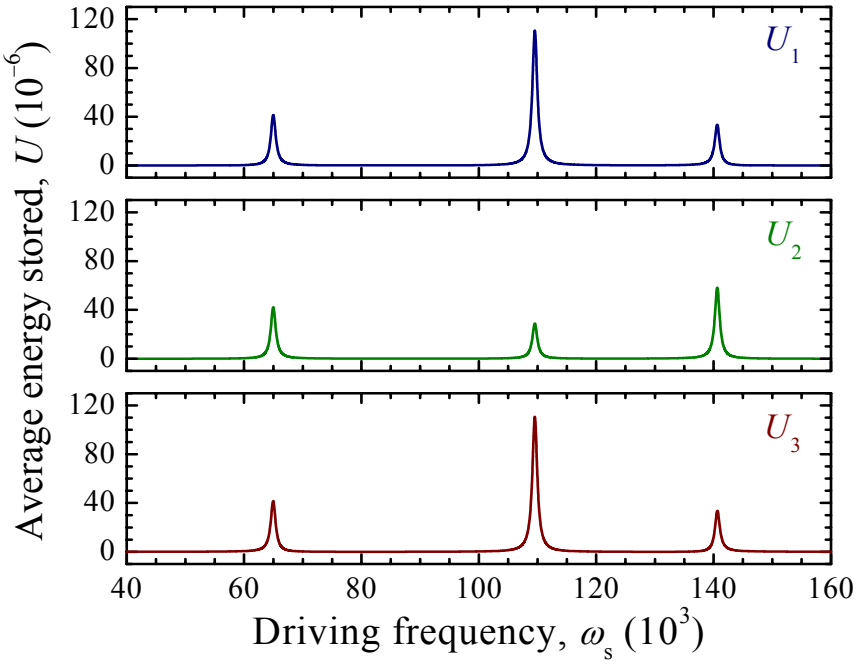

Figure 2 Energy, in micro-Joules, stored in each of the three coupled LRC circuits as a function of the oscillator frequency, ω_s, in Hz, for the following values of the circuit parameters: $L_1 = L_2 = L_3 = 1$ mH, $R_1 = R_2 = R_3 = 1\ \Omega$, $C_1 = 1/6.5$ μF, $C_2 = 1$ μF, $C_3 = 1/6.5$ μF, $C_{12} = 1/5.5$ μF, and $C_{23} = 1/5.5$ μF and a driving voltage of 1 V RMS.

Figure 2 clearly shows this resonance splitting. The upper, middle and lower figures show respectively the average energy stored in circuits 1, 2, and 3 as a function of frequency. The central resonance is at the common circuit frequency which for the chosen circuit parameters is 109.54 kHz. For the same values of L and R a single LRC circuit tuned to any of the three frequencies shown, driven with 1 V RMS would store 500 μJ of energy, considerably larger than that of any of the three circuits at any resonance. A single circuit would have a Q of ωL/R which at the center frequency is 109.45. In the present case where we have chosen $L_1 = L_2 = L_3$ and $R_1 = R_2 = R_3$ the Q of all three resonances of the three coupled circuits will also be given by ωL/R and will thus be the same as that of a single circuit at each of those frequencies. If the L/R ratios for the three circuits are different, the Q values for the coupled circuit resonances will always be smaller than that of a single circuit with the largest value of L/R. If ω_{11}, ω_{22}, and ω_{33} are the resonant frequencies of the individual circuits given by

$$\omega_{11}^2 = \frac{1}{L_1}\left(\frac{1}{C_1}+\frac{1}{C_{12}}\right),\ \omega_{22}^2 = \frac{1}{L_2}\left(\frac{1}{C_2}+\frac{1}{C_{12}}+\frac{1}{C_{23}}\right),\ \omega_{33}^2 = \frac{1}{L_3}\left(\frac{1}{C_3}+\frac{1}{C_{23}}\right) \qquad (1)$$

and

$$\omega_{12}^4 = \frac{1}{L_1 L_2 C_{12}^2}\ \text{, and}\ \omega_{23}^4 = \frac{1}{L_2 L_3 C_{23}^2} \qquad (2)$$

are the resonant frequencies associated with the coupling capacitors, the resonant frequencies of the three coupled circuits are given by

$$(\omega_{11}^2-\omega^2)(\omega_{22}^2-\omega^2)(\omega_{33}^2-\omega^2) = (\omega_{11}^2-\omega^2)\omega_{23}^4 + (\omega_{33}^2-\omega^2)\omega_{12}^4\,. \qquad (3)$$

The sum of the three solutions to equation 3 are related to the three individual resonant frequencies by

$$\sum_i \omega_i^2 = \omega_{11}^2 + \omega_{22}^2 + \omega_{33}^2 \ . \qquad (4)$$

Similarly, if we designate the loss factors for the three separate circuits by γ_{11}, γ_{22}, and γ_{33}, then the loss factors for the three resonances are related to those of the individual circuits by

$$\sum_i \gamma_i = \gamma_{11} + \gamma_{22} + \gamma_{33} \ , \qquad (5)$$

where $\gamma_{ii} = R_i/L_i$.

It can also be readily shown that the three loss factors, γ_i, all lie between the minimum and maximum values of the γ_{ii}. Therefore none of the resonances of the three coupled LRC circuits will have a loss factor less than that of the value for the least lossy of the individual circuits, and thus the coupled circuits will not have a Q larger than that of the highest Q individual circuit. In addition, it can be shown that the sum of the total energy that can be stored in all three circuits together at all three resonant frequencies is equal to the energy that can be stored in a single circuit with the same values of L and R. Figure 3 is a plot of the stored energy in each of the three coupled circuits as a function of the coupling capacitance keeping the center frequency constant.

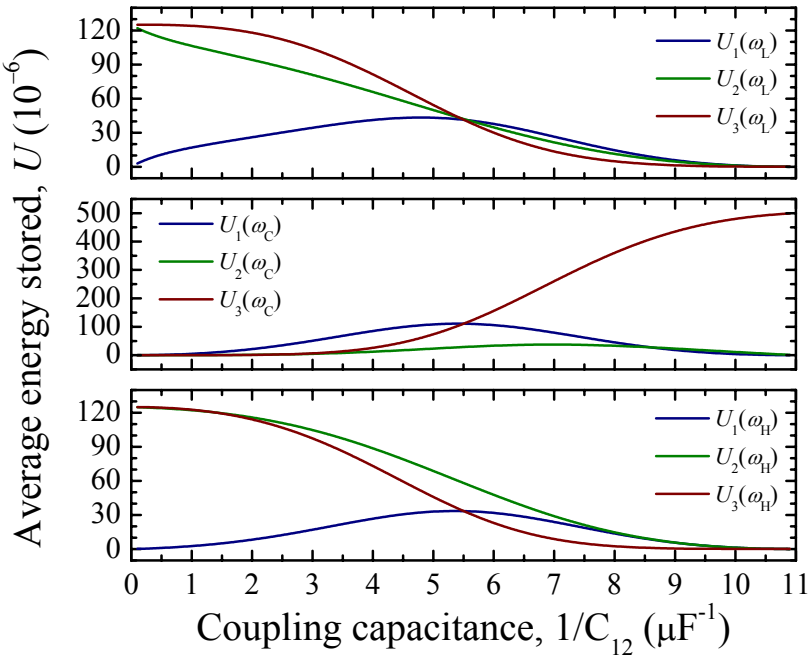

Figure 3 Plot of the energy stored in each of the three coupled circuits as a function of the coupling capacitance with the center frequency held constant. The parameters are the same as in Figure 2 except that $1/C_{12}$ is allowed to vary keeping $(1/C_{12}+1/C_{23})$ constant at the value of Figure 2.

The upper, middle and lower plots in Figure 3 show the stored energy in each of the three circuits at the lowest, center and highest resonant frequencies respectively. (The plot shown in Figure 2 corresponds to a coupling capacitance in the middle of Figure 3.) Figure 3 shows that for small values of $1/C_{12}$, which correspond to large values of $1/C_{23}$,

more energy is stored in circuits 2 and 3 than in circuit 1. This can be understood if one considers that the strength of the coupling between the circuits is proportional to the inverse of the respective coupling capacitances. Thus the left hand side of Figure 3 corresponds to strong coupling between circuits 3 and 2 but weak coupling between circuits 2 and 1. Thus one would expect that the bulk of the energy would be concentrated in circuits 3 and 2 as seen in Figure 3. Furthermore it is seen that there is virtually no energy in the central resonance at low values of $1/C_{12}$. In this region of the plot the tri-circuit configuration is behaving as though there were only two circuits connected and circuit 1 is effectively isolated. When two circuits are coupled the resonance splits into two, one at higher and one at lower frequency than that of the original circuits. This is exactly what is happening here. Similarly the right hand side of Figure 3 corresponds to weak coupling between circuits 3 and 2 but strong coupling between circuits 2 and 1. Thus on the right hand side of Figure 3 all of the energy is stored in circuit 3, which is behaving like a single circuit with a resonance at the center frequency. Very little is coupled to circuits 2, and 1 and all of the energy is in the center frequency resonance.

Figure 4 is a plot of the total energy stored in all three coupled circuits as a function of the coupling capacitance. Figure 4 shows that the total energy that can be stored in all of the coupled circuits together at all frequencies together is independent of the coupling capacitances and equal to 500 μJ, which is that of a single circuit with the same loss factor as the individual coupled circuits.

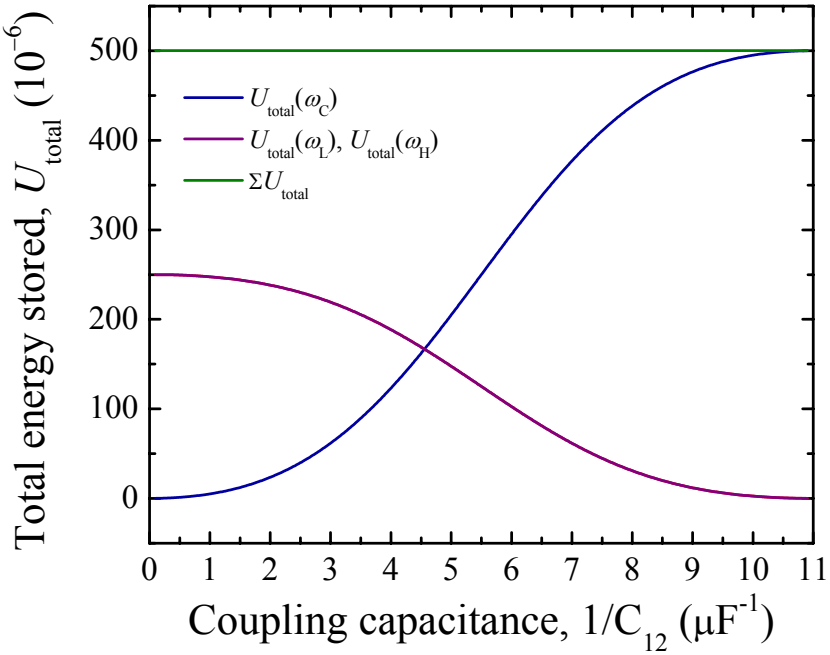

Figure 4 Total energy stored in all three coupled circuits as a function of the coupling capacitance and the sum of these for the three resonant frequencies.

Again Figure 4 shows that when the coupling between circuits 1 and 2 is weak, and the coupling between circuits 2 and 3 is strong, left hand side of Figure 4, virtually all of the energy, which is concentrated in circuits 2, and 3, is in the higher and lower split-off resonances with very little in the center frequency. Likewise at the right hand

side of Figure 4 where the coupling between circuit 3 and circuit 2 is weak, all of the energy is in circuit 3 and at the center frequency appropriate for a single circuit.

The conclusion of this section of the work is that although coupled LRC RF circuits evidence a splitting of the resonant frequency into as many branches as there are coupled circuits no enhancement in energy storage capacity or improvement in Q occurs. We have already seen that such enhancements and improvements do occur in the case of coupled ring resonators[1-3].

3. Coupled optical resonators

The next investigation undertaken was that of coupled optical Fabry-Perot cavities and optical ring resonators. The mathematical analysis of the Fabry-Perot and optical ring resonator situations is essentially identical. In the following we will refer to these generically as coupled optical resonators, dropping the distinction. The principal difference between coupled optical resonators and coupled LRC circuits is that the wavelength of the oscillation can not be ignored in the case of the optical resonators while it can be, and is, ignored in the case of the RLC circuits. All dimensions in the LRC circuit are considered to be small compared to the wavelength of the resonant frequency. In the above case that wavelength is approximately 3 km. So long as this is very large compared to dimensions of the circuits the analysis should be valid. In the case of the optical resonators the element dimensions are comparable to the wavelength of the oscillation and the resonator dimensions as well as the other resonator parameters will control the behavior of the coupled elements. Figure 5 is a representation of three coupled Fabry-Perot structures.

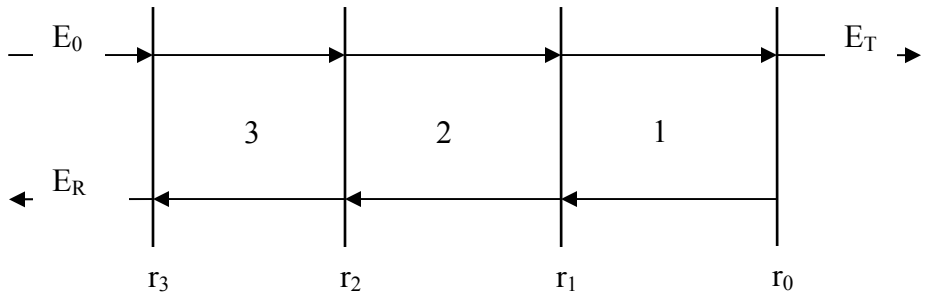

Figure 5 Diagram of triply coupled Fabry-Perot cavities

In Figure 5 electromagnetic energy is incident from the left as E_0. A portion of that energy is reflected from mirror 3, with reflectance r_3, as E_R and a portion transmitted to mirror 2 and so forth. If none of the mirrors are perfectly reflecting there will be transmitted energy represented as E_T. The analysis of coupled Fabry-Perot structures, as the one shown in Figure 5, must take into account not only the magnitude and phase of the reflected and transmitted energy at each mirror but also the optical path length of each cavity. The analysis proceeds virtually identically to that in reference 1 for the ring resonators. The following analysis applies to coupled optical ring resonators as well as to coupled Fabry-Perot resonators and we will adopt the language of the optical resonators.

The analysis pertains to the Fabry-Perot coupled resonators as well. In the following we will emphasize the differences between this work and that of reference 1 as well as our conclusions.

The first difference between this work and that of reference 1 is that the optical reflection coefficients are allowed here to be complex whereas in reference 1 they are considered to be real. In general one can write the complex reflection and transmission coefficients as $r = r_0 e^{i\phi_r}$ and $t = t_0 e^{i\phi_t}$. An analysis of the reflection determines that *r* and *t* can be written as

$$r = r_0^2 \pm i r_0 \cdot t_0 \text{ and } t = t_0^2 \mp i t_0 r_0 \tag{6}$$

where r_0 and t_0 are real and positive. It is easy to show from this that

$$\phi_t = \phi_r \pm \pi/2. \tag{7}$$

In reference 1, ϕ_r is set equal to 0, and $\phi_t = \pi/2$ so equation 7 is preserved but *r* is considered to be real. Fortunately one can absorb the phase shift of the reflections in the phase related to the cavity optical path length so that none of the results in reference 1 are negated so long as one remembers that these phase shifts are included in the path lengths. In the remainder of this report we will follow the notation in reference 1 in which *r* and *t* are real and the relationship expressed in equation 7 is incorporated directly in the equations.

The second difference is that reference 1 considered primarily optical cavities of the same size and thus the same phase shift. This results in a large splitting of the optical cavity modes, similar to the case of the coupled LRC circuits, which is a major conclusion of reference 1. Reference 1 also examined the amplification, or magnification, of the optical energy which can occur when multiple cavities are appropriately coupled. This result represents a significant difference between coupled optical cavities and coupled LRC circuits where no such magnification is observed. However, because only coupled cavities with the same phase shift were considered, reference 1 observes somewhat limited enhancement in the cavity resonance *Q* and energy storage capacity particularly for even numbers of coupled cavities. It was determined in this work that higher *Q* and larger energy storage can be achieved by introducing a π phase shift between the cavities. Nevertheless it was also determined that *Q* and energy storage is still largest for a single optical cavity provided that optimum cavity size and coupling reflectivity can be achieved. However, in the case where these optimum factors can not be achieved it may be possible to achieve larger energy storage in coupled cavities and a larger *Q* than can be achieved in a single cavity. This is another, and quite significant, difference between the results of the analysis on coupled optical resonators and LRC circuits.

We will start with the analysis of a single optical resonator. Consider in Figure 5 that the configuration consists of a single cavity, sections 3 and 2 don't exist, and that r_0=1 so no energy is transmitted. The ratio of the optical power stored in cavity 1 to the incident power is given by

$$M_{11} = \frac{t_1^2 a_1^2}{(1 - r_1 a_1)^2 + 4 r_1 a_1 \sin^2\left(\frac{\phi_1}{2}\right)} \tag{8}$$

where t_1 is the transmission and r_1 is the reflectance of the first mirror, a_1 represents the possible loss in the first cavity, $a_1 = 1$ for a lossless cavity, and ϕ_1 is the round-trip phase change in the cavity. The maximum energy stored occurs at the maximum value of M_{11} which occurs at $\phi_1 = \pi n$. In this case

$$M_{11\max} = \frac{(1-r_1^2)a_1^2}{(1-r_1a_1)^2} \tag{9}$$

and

$$Q_{11} = \frac{\sqrt{r_1a_1}}{(1-r_1a_1)} \tag{10}$$

where $t_1^2 = 1-r_1^2$. If the value of r_1 can be adjusted, the optimum values of M_{11} and Q_{11} are obtained when $r_1 = a_1$. In this case

$$M_{11opt} = \frac{a_1^2}{(1-a_1^2)} \tag{11}$$

and

$$Q_{11opt} = \frac{a_1}{(1-a_1^2)}. \tag{12}$$

It turns out that this is the best that can be done when the magnification and Q factors are limited purely by the cavity losses. If, however, the limitation is due in part to a limited reflectivity then enhanced magnification and improved Q can be obtained through the use of multiple cavities. This is shown quite convincingly in reference 1. Reference 1 shows that greatly enhanced values of magnification can be achieved particularly for odd numbers of coupled resonators. This is due to the fact that reference 1 considers zero phase difference in the optical path lengths of the coupled cavities.

In the present work we will consider two coupled cavities as basically most of the effects can be seen in this configuration. In this case simply consider that cavity 3 in Figure 5 is missing and again that $r_0 = 1$. For two cavities equation 8 becomes rather more complicated. Considering the magnification achieved in cavity 1 of a two-cavity coupled system one obtains, instead of equation 8

$$M_{21} = \frac{t_2^2t_1^2a_2a_1^2}{A + B\sin^2\left(\frac{\phi_1}{2}\right) + C\sin^2\left(\frac{\phi_2}{2}\right) + D\sin^2\left(\frac{\phi_1+\phi_2}{2}\right) + E\sin^2\left(\frac{\phi_1-\phi_2}{2}\right)} \tag{13}$$

where

$$\begin{aligned} A &= \left[(1-r_1a_1) + r_2a_2(a_1-r_1)\right]^2 \\ B &= 4r_1a_1(1+r_2^2a_2^2) \\ C &= 4r_1r_2a_2(1+a_1^2) \\ D &= -4r_2a_2a_1 \\ E &= -4r_1^2r_2a_1a_2 \end{aligned} \tag{14}$$

For the magnification achieved in cavity 2 of a two-cavity coupled system we obtain

$$M_{22} = \frac{t_2^2 a_2^2 \left[(a_1 - r_1)^2 + 4 r_1 a_1 \sin^2\left(\frac{\phi_1}{2}\right) \right]}{A + B\sin^2\left(\frac{\phi_1}{2}\right) + C\sin^2\left(\frac{\phi_2}{2}\right) + D\sin^2\left(\frac{\phi_1+\phi_2}{2}\right) + E\sin^2\left(\frac{\phi_1-\phi_2}{2}\right)} \tag{15}$$

For $\phi_2 = \phi_1$ equations 13 and 15 simplify somewhat. Figures 6 and 7 are plots of the values of M_{21} and M_{22} as functions of ϕ_1, where $\phi_2 = \phi_1$, showing the expected resonance splitting. The magnitude of this splitting is a function of the various cavity parameters.

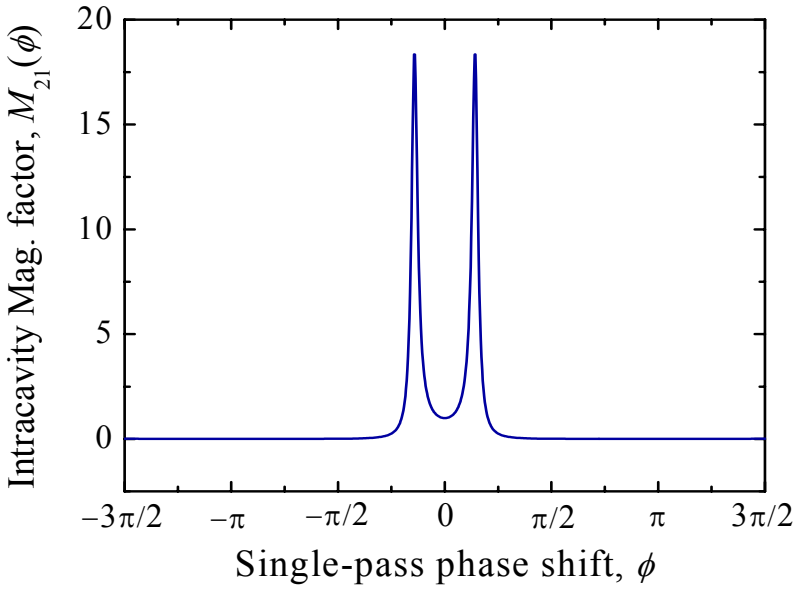

Figure 6 Value of M_{21} versus ϕ_1 for $\phi_2 = \phi_1$. In this plot we have used $r_1 = r_2 = 0.9$, and $a_1 = a_2 = 0.999$.

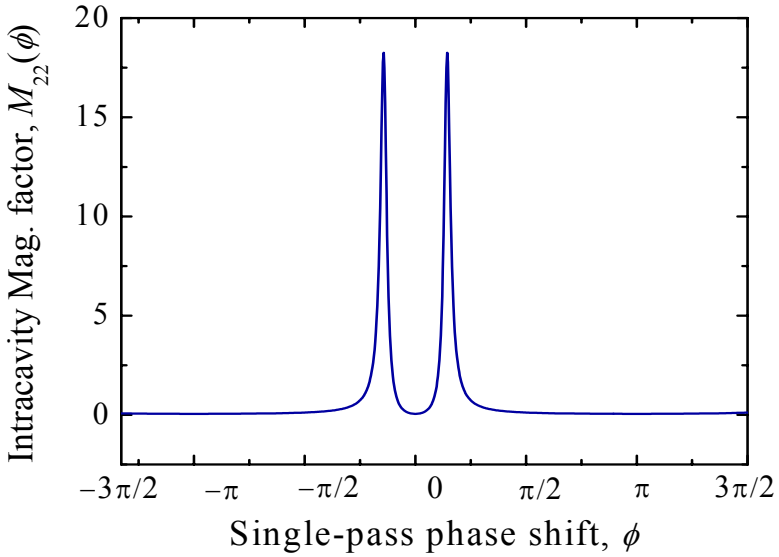

Figure 7 Value of M_{22} versus ϕ_1 for $\phi_2 = \phi_1$ and the same parameters as in Figure 6

The magnitude of the phase shift is given by

$$\cos\phi = \frac{r_1(a_1 + r_2 a_2)(1 + r_2 a_2 a_1)}{4 r_2 a_1 a_2} \tag{16}$$

As the right hand side of equation 16 approaches 1 with increasing values of reflectance, the two resonances merge into one at $\phi = 2\pi n$. For larger values the resonance remains at $\phi = 2\pi n$. In this situation M_{21} becomes

$$M_{21\max} = \frac{t_1^2 t_2^2 a_1^2 a_2}{\left[(1 - a_1 r_1) + a_2 r_2 (a_1 - r_1)\right]^2} \quad (\text{for } \phi_2 = \phi_1)\,. \tag{17}$$

Again we can examine the optimum value of M_{21} by maximizing with respect to r_2 and r_1. This results in $r_1 = a_1$ and $r_2 = 0$ in which case

$$M_{21opt} = \frac{a_2 a_1^2}{(1 - a_1^2)} = M_{11opt} \cdot a_2 \quad . \tag{18}$$

Since $a_2 \le 1$ $M_{21opt} \le M_{11opt}$. Furthermore if we ignore cavity losses by setting a_1 and a_2 equal to one, equation 17 becomes

$$M_{21\max} = \frac{(1 + r_1)}{(1 - r_1)} \cdot \frac{(1 - r_2)}{(1 + r_2)} \qquad (\text{for } \phi_2 = \phi_1) \tag{19}$$

whereas for the single circuit, under the same circumstances we would have

$$M_{11\max} = \frac{(1 + r_1)}{(1 - r_1)}\,. \tag{20}$$

This is the same result as that obtained in reference 1 where the ratios continue to invert from cavity to cavity so that, for example

$$M_{31\max} = \frac{(1 + r_1)}{(1 - r_1)} \cdot \frac{(1 - r_2)}{(1 + r_2)} \cdot \frac{(1 + r_3)}{(1 - r_3)} \qquad (\text{for } \phi_2 = \phi_1) \tag{21}$$

etc. It should be noted, however, from equations 11 and 18, that the optimized magnification for the lossless case is infinite.

If we do not set $\phi_1 = \phi_2$ we get different results. For example, if we set $\phi_2 = \phi_1 + \pi$ and plot equations 13 and 15 versus ϕ_1, we get the results shown in Figures 8 and 9 using otherwise the same cavity parameters as in Figures 6 and 7. In this case we see that for M_{21} and M_{22} there is no splitting of the resonance and that the magnitude of the $\phi_1 = 0$ resonance for M_{21} in Figure 8 is considerably larger than that of the split resonances in Figure 6. For $\phi_2 = \phi_1 + \pi$ the expression for $M_{21\max}$ in equation 17 is changed to

$$M_{21\max} = \frac{t_1^2 t_2^2 a_1^2 a_2}{\left[(1 - a_1 r_1) - a_2 r_2 (a_1 - r_1)\right]^2} \quad (\text{for } \phi_2 = \phi_1 + \pi) \tag{22}$$

and the expression for $M_{22\max}$ in equation 19 is changed to

$$M_{22\max} = \frac{t_2^2 a_2^2 (a_1 - r_1)^2}{\left[(1 - a_1 r_1) - a_2 r_2 (a_1 - r_1)\right]^2} \quad (\text{for } \phi_2 = \phi_1 + \pi) \tag{23}$$

Note that the only change is in the sign of $a_2 r_2$ which, however, as we will see, makes a big difference. Nevertheless, if we again optimize $M_{21\max}$ by maximizing with respect to r_1 and r_2 we get the same results as we did for equation 17, namely equation 18 and a

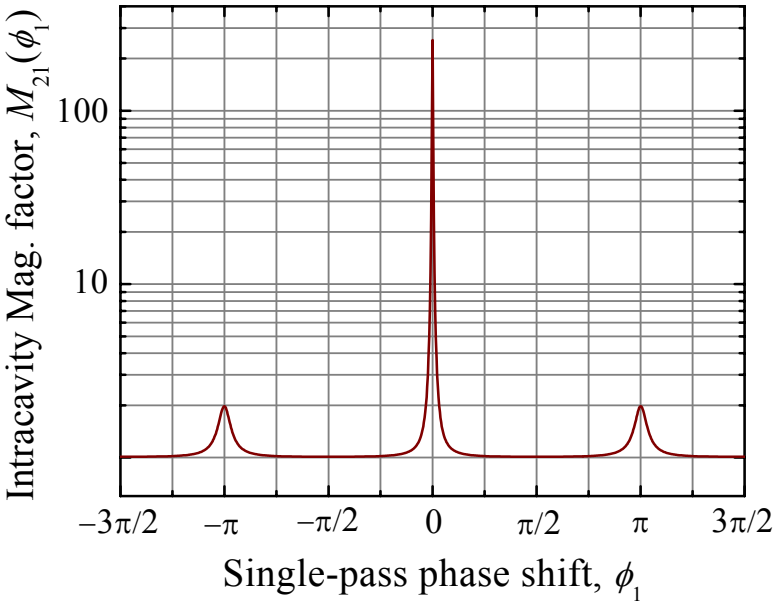

Figure 8. Value of M_{21} versus ϕ_1 for $\phi_2 = \phi_1 + \pi$ using otherwise the same cavity parameters as in Figure 6 Note that Figure 8 is plotted on a log scale with 1 added so as to avoid the – infinity for $M_{21\max} = 0$.

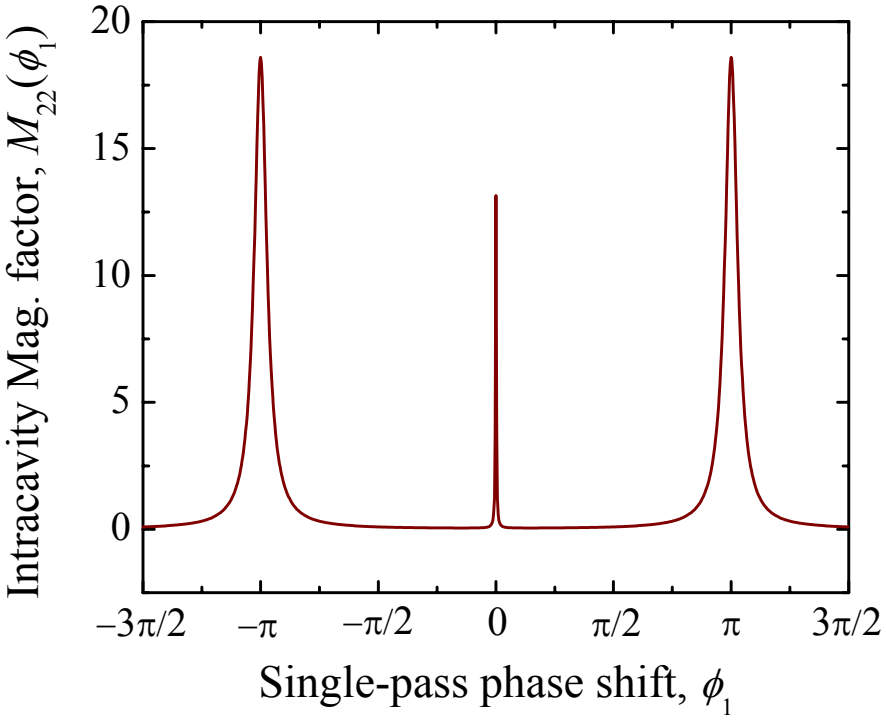

Figure 9. Value of M_{22} versus ϕ_1 for $\phi_2 = \phi_1 + \pi$ using otherwise the same cavity parameters as in Figure 6

single circuit is still superior. However, the results for the lossless case with limited r_1 and r_2 are significantly different. Equation 22 becomes

$$M_{21\max} = \frac{(1+r_1)}{(1-r_1)} \cdot \frac{(1+r_2)}{(1-r_2)} \qquad (\text{for } \phi_2 = \phi_1 + \pi) \tag{24}$$

and equation 23 becomes

$$M_{22\max} = \frac{1+r_2}{1-r_2}. \qquad (\text{for } \phi_2 = \phi_1 + \pi) \tag{25}$$

Each additional cavity adds to the magnification of $M_{21\max}$ if this relative phase relation is continued.

We can use equations 22 and 23 to calculate the values of $M_{21\max}$ and $M_{22\max}$. This results in $M_{21\max} = 254.63$ and $M_{22\max} = 13.13$ in good agreement with Figures 8 and 9. These can be compared to $M_{11\max} = 18.64$ given by equation 9 and the same parameters. If instead we were to use the lossless equations 24 and 25 we would obtain $M_{21\max} = 361$ and $M_{22\max} = 19$ and equation 11 gives $M_{11\max} = 19$.

As can be seen, the magnification is greatly enhanced by the addition of a second resonant cavity so long as the parameters are not optimized. It is also useful to determine the effect the addition of a second cavity has on the quality factor, Q. Examination of Figures 8 and 9 indicate that Q can be quite large. The value of Q corresponding to $M_{21\max}$ is given by

$$Q_{21} = \frac{\sqrt{r_1(a_1(1+a_2^2r_2^2) - a_2r_2(1+a_1^2)) + 4r_2a_1a_2}}{\left((1-a_1r_1) - a_2r_2(a_1 - r_1)\right)} \qquad (\text{for } \phi_2 = \phi_1 + \pi). \tag{26}$$

With $a_1 = a_2 = 0.999$ and $r_1 = r_2 = 0.9$ as above, equation 26 gives $Q_{21} = 143.7$ compared to a value of Q_{11} from equation 10 of $Q_{11} = 9.40$. For the same values of reflectivity, the lossless cases give $Q_{21} = 171.0$ and $Q_{11} = 9.49$. And, as for the magnifications, the quality factors, Q, can be greatly enhanced for the two-cavity structure over that of a single cavity. However they remain below those of the optimum values for a single cavity with a loss factor of 0.999. For this case we would obtain $M_{11\text{opt}} = 499.25$, $Q_{11\text{opt}} = 499.75$, given by equations 11 and 12 respectively, and $M_{21\text{opt}} = 498.75$, and $Q_{21\text{opt}} = 499.75$ given by equations 22 and 26 respectively. Values are collected in Table I. (for $\phi_2 = \phi_1 + \pi$)

	M_{21}	Q_{21}	M_{11}	Q_{11}
Given Values	254.63	159.63	18.64	9.40
Lossless	361.00	174.28	19.00	9.49
Optimum	498.75	499.75	499.25	499.75

Table I

It is useful to attempt to get some insight into these results. First, for the case where we consider that $\phi_2 = \phi_1$, we see that the single-cavity resonance is split into two. This is similar to what one experiences in the case of two coupled LRC circuits. In the case of two identical coupled LRC circuits the higher and lower frequency resonances correspond respectively to in-phase and out-of-phase coupling through the coupling capacitor. When the coupling is out of phase, which occurs for the lower frequency resonance, currents in the two circuits flow in opposite directions through the coupling capacitor, and no total current flows through this capacitor. In this case no voltage appears across the capacitor and this capacitance is effectively eliminated from the circuit. As the capacitors are in series, the elimination of one increases the overall

effective capacitance lowering the resonant frequency. The opposite is the case for the higher resonance where the coupling is in phase, the coupling capacitor is effectively included twice in series so the overall capacitance is lowered and the resonance frequency is raised.

In the case of the coupled optical cavities there is an effective π/2 phase shift in transmission through the cavity-to-cavity coupling as indicated in equation 7. Cavity-to-cavity transmission in the in-phase resonance essentially goes through this coupling interface twice increasing the effective overall optical path length and reducing the resonant frequency. The out-of-phase resonance essentially does not go through the coupling interface at all reducing the effective overall optical path length and increasing the resonant frequency. Let us re-examine equation 16 for the line splitting. Equation 16 indicates that the line splitting vanishes as the reflectances become large, and consequently as the transmission through the coupling interfaces becomes very small. In this case the resonators are only weakly coupled and very little of the energy goes through the coupling interface. Little of the energy suffers the phase shift due to transmission and the splitting vanishes. In the opposite extreme as the reflectances become very small virtually all of the energy goes through the coupling interface and the splitting becomes very large and can approach π. In this case the difference in phase shift between the in-phase resonance and the out-of-phase resonance cases is twice π/2 or π as given by equation 16. The interference between the waves results in a limitation on the magnification such that the resonant magnifications for two coupled resonant circuits are about the same as for a single resonant cavity with the same parameters.

In the case where $\phi_2 = \phi_1 + \pi$ the waves are shifted by π/2 during each half-circuit so the waves are effectively out of phase with each other by π/2 and do not constructively or destructively interfere resulting in no splitting. This lack of interference and splitting allows for the greatly improved magnification and cavity *Q*.

4. Conclusions

In this work we showed for the LRC case that coupling two or more resonant circuits together can result in resonant line splitting and that electromagnetic energy can be stored in any of the coupled circuits, depending on the circuit parameters, but that no enhancement in the magnitude of either the stored energy or the *Q* of the resonance can be achieved over that of a single resonant circuit. In this case the circuit resonance frequencies only depend on the circuit parameters namely the values of the circuit inductances and capacitances. In the case of the coupled optical cavities we can also observe resonant line splitting and that electromagnetic energy can be stored in any of the coupled cavities. In contrast to the LRC case, we can also get a substantial enhancement of the magnitude of the stored energy and the effective cavity *Q* over that of a single resonator provided these factors are limited by the coupling between the cavities. However, when this coupling can be optimized we see that the energy storage and *Q* of a single cavity is superior to that of the coupled cavities. The advantages of the coupled resonators come in their ability to show line splitting, enhanced energy storage, and high *Q* even when the cavity-to-cavity coupling is limited. Under these circumstances one should also be able to obtain reduced laser thresholds through the use of coupled optical cavities wherein at least one of them displays gain.

ACKNOWLEDGMENTS

I would like to sincerely acknowledge and thank NASA for the support of the SFFP program. I would also like to sincerely thank the Marshall Space Flight Center and Dr. David D. Smith for the opportunity of working on this very interesting research program. The time has been far too short and has passed far too quickly. Moreover my special thanks go to Mr. Hongrok Chang without whose support and help far less would have been accomplished. Mr. Chang has been a constant companion in this work checking my calculations, making those of his own, and providing excellent advice as to how to proceed; and, not the least, creating all of the figures in this report.

REFERENCES

1. Smith, David D., Chang, Hongrok, and Fuller, Kirk A., *Whispering-gallery mode splitting in coupled microresonators*, J. Opt. Soc. Am. B 10887 (2003)
2. Smith, David D., Witherow, William K., and Fuller, Kirk A., *Coupled-Resonator-Enhanced Sensor Technologies*, NASA MSFC Center Director's Discretionary Fund – FY 2003, Project Number: 03-17.
3. Rosenberger, A. T., and Naweed, Ahmer, *Induced Transparency and Related Effects in Coupled Whispering-Gallery Microresonators*, to be published.